05.05.2008

Coma-Free Operation Mode of the SAXES spectrometer /Technical Report No. SLS-SPC-TA-2008-309/

V.N. Strocov
Th. Schmitt
L. Patthey

Abstract: An operation mode of the SAXES spectrometer identically free of coma aberrations is identified. This mode brings an improvement of resolution by a factor of ~2 compared to operation at arbitrary incidence angles. Moreover, it allows increase of the spectrometer aperture and thus throughput without any significant loss of resolution. A software tool is developed to find the coma-free spectrometer settings.

Paul Scherrer Institut
CH-5232 Villigen-PSI
Switzerland

The optical scheme of the SAXES spectrometer installed at the ADRESS beamline is based on spherical VLS grating. The grating equation $\cos\alpha+\cos\beta=Nk\lambda$ determines the relation between the incident angle α and exit angle β (the grazing angle notation). The value of α can be used as an addition degree of freedom to minimize the aberrations. Here, we demonstrate that optimization of α in spherical grating VLS spectrometers such as the SAXES allows not only minimization but complete cancellation of the coma aberrations similarly to the Rowland circle geometry.

The effect of α on the spectrometer aberrations was investigated with ray tracing simulations using a specialized code written in Matlab. To accelerate the calculations and achieve efficient sampling of α, the simulations were performed in two dimensions in the dispersive plane and used a point source with angular divergence restricted to this plane. The resulting lineshape was convoluted with a Gaussian describing additional broadening due to finite spot size, slope errors of the grating and CCD spatial resolution.

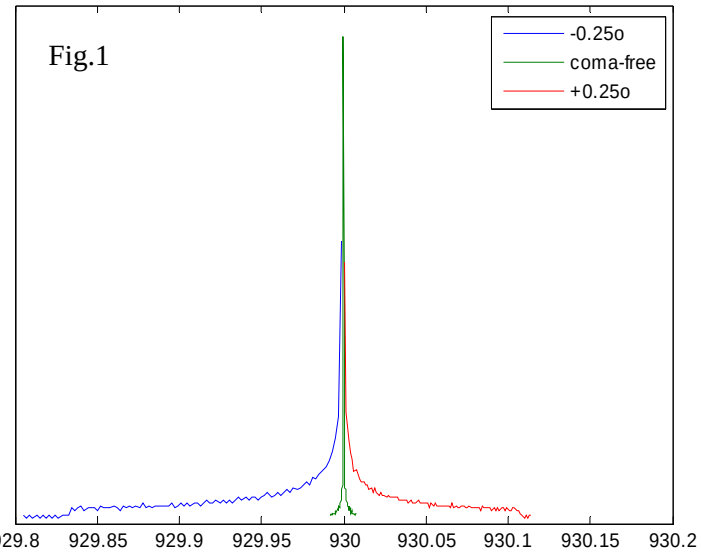

Fig.1

The coma cancellation is illustrated by ray tracing simulation in Fig. 1 showing the image on the CCD detector obtained for the SAXES spectrometer (point source, no Gaussian broadening factors, energy 930 eV, mask 1 mm, grating in 1000 mm from the source, CCD at the focal distance, CCD inclination angle 20^o). At the optimal grazing angle $\alpha_{opt}=1.36^o$ the image is identically coma free, whereas those at $\pm0.25^o$ already show strong coma with its characteristic asymmetric shape and long tail towards lower or higher energies. Note that all images are produced in their own focal points at different exit arm lengths. α_{opt} can be identified by zero skewness (asymmetry) of the image. It certainly depends on energy, diffraction order (the same calculation for zero order return $\alpha_{opt}=0.93^o$) and entrance arm length, but is almost insensitive to illumination of the grating (mask).

These results were verified with a generic ray tracing code PHASE (J. Bahrdt and U. Flechsig) standard in SLS. We used the same set of parameters (except that for simplicity the CCD plane perpendicular to the ray). The top panels in Fig.2 show the results obtained for same point source with the angular divergence restricted to the dispersive plane. The grazing angle was set to α_{opt}. The lineshape is identical to Fig.1, narrow and coma-free. Deviations from α_{opt} immediately resulted in piling up of the coma tails (not shown here). The bottom panels in Fig. 2 show the results of simulations performed a point source having angular divergence in both meridional and sagittal plane. The image stays narrow and identically coma-free. The shoulder on the right side of the peak is not a sign of the coma, but appears due the curvature of the image in the sagittal direction.

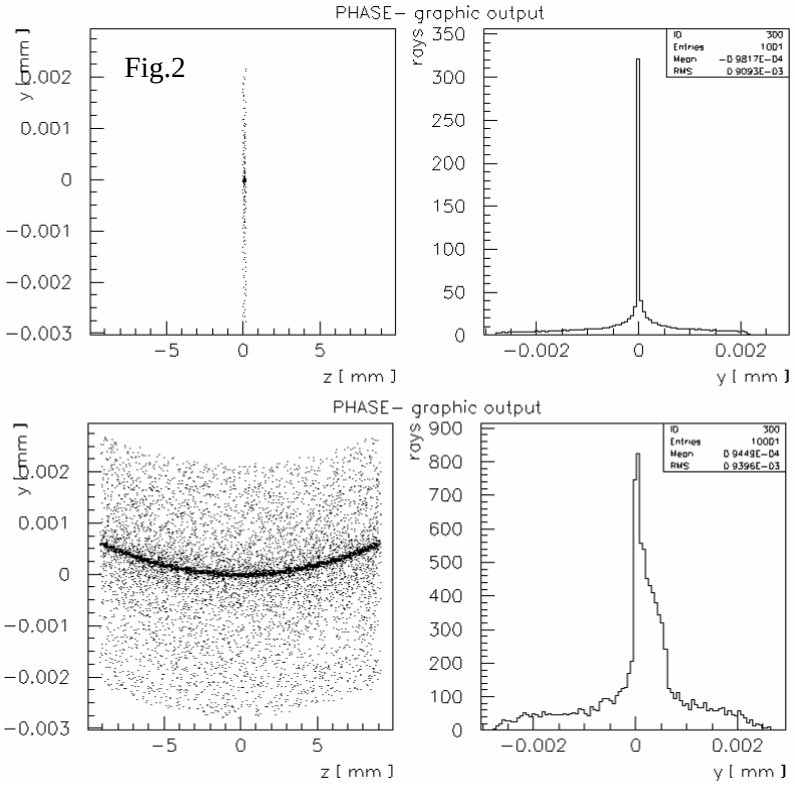

Other contributions to the image broadening (Gaussian broadening due to source size, grating slope errors and spatial resolution of the detector) make the aberrations less pronounced. Fig. 3 shows angular dependence of their FWHM calculated with typical SAXES operation parameters (indicated in the inset) as well as their combined FWHM. The latter slightly decreases towards more grazing angles. The combined effect of the above Gaussian broadening factors on the images in Fig. 1 is illustrated by simulation in Fig. 4. The coma

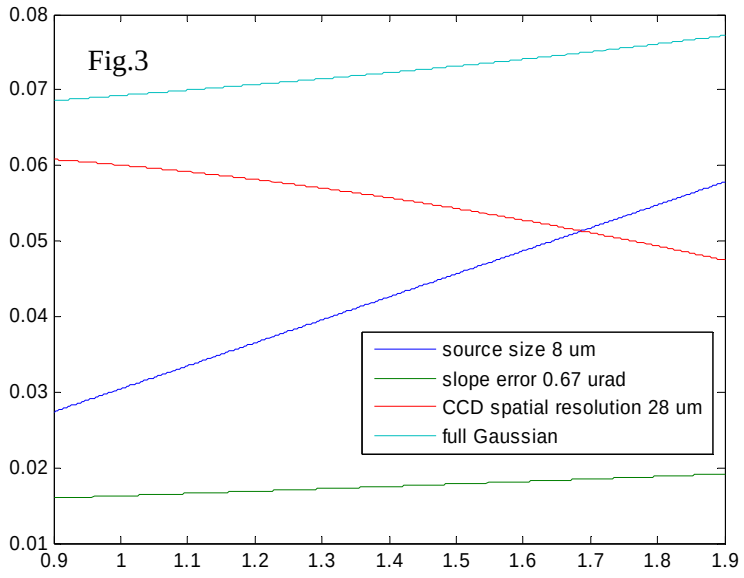

aberrations creep into the broadened images as asymmetric lineshape and increased FWHM.

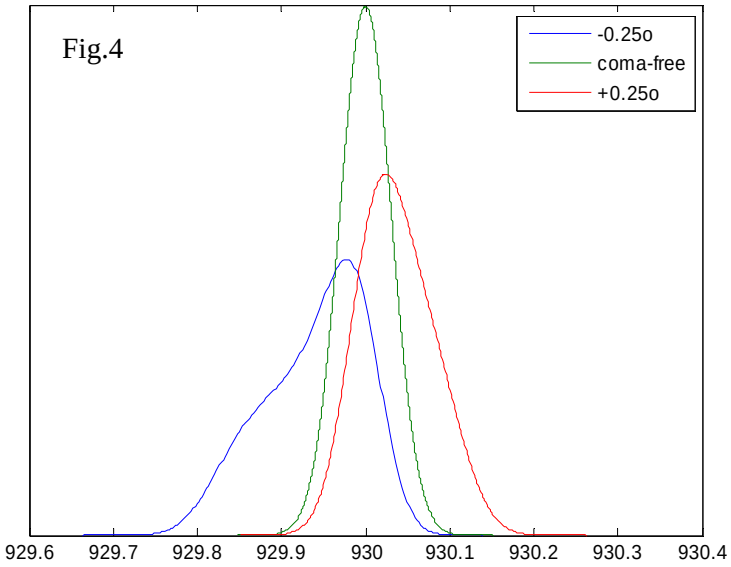

Fig. 5 shows the angular dependence of the combined linewidth FWHM incorporating both aberrations and Gaussian broadening factors. Despite the broadening, it preserves a pronounced minimum centered at α_{opt} with a deviation <0.01°. Operation of the spectrometer at this coma-free grazing angle brings *improvement in resolution by a factor about 2* compared to operation at arbitrary angles.

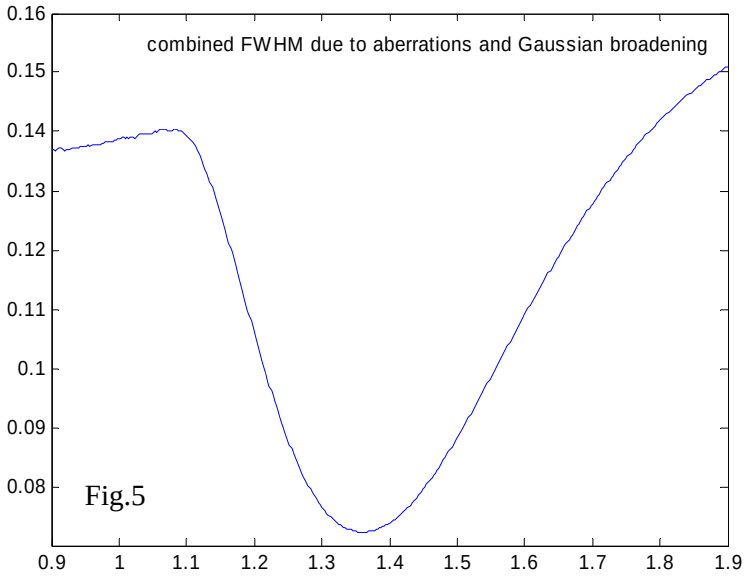

Finally, Fig. 6 shows the above angular dependence of the combined linewidth FWHM calculated for different grating illuminations (average over the shown angular span). As expected from the quadratic dependence of coma aberrations, the FWHM minimum corresponding to the coma-free conditions is fairly broad at small illuminations and becomes steep (~0.1° wide) at large illuminations. Exactly at the coma-free angle we even observe a local maximum piling up at large illuminations. It manifests higher-order aberrations. In any case,

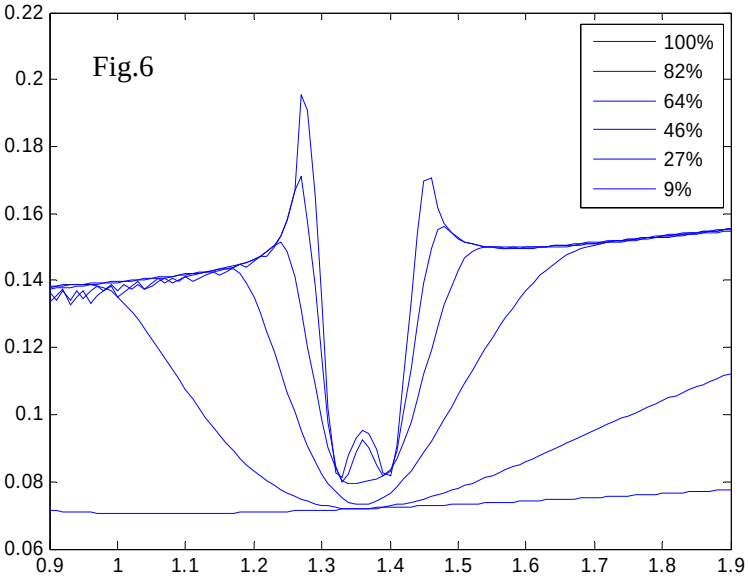

degradation of resolution towards 100% illumination is only ~30% in the coma-free conditions as compared to more than twice at arbitrary angles. Therefore, operation of spectrometer in the coma-free mode allows opening the aperture towards full illumination thus dramatic *increase of flux* without any significant loss of resolution.

Determination of the coma-free angle has been implemented in a standalone application shown in Fig. 6. The code is written in Matlab and platform independent. It performs explicit ray tracing in the dispersion plane, starting from the point source at the sample position and propagating towards the CCD image plane where the lineshape is yielded. The coma-free α_{opt} is automatically determined as delivering zero lineshape skewness. Broadening due to the source size, grating slope errors and CCD spatial resolution is introduced by Gaussian convolution. The code displays the resulting lineshape, as well as the corresponding geometry and resolution parameters. An additional analysis window shows the resolution dependence on the grazing angle or exit arm, which allows optimization of the spectrometer settings under its mechanical constraints. By virtue of code vectorization the calculations are performed in a fraction of second. Similar analysis using generic ray tracing software like SHADOW would be far more laborious due to necessity of manual setup of the computational parameters.

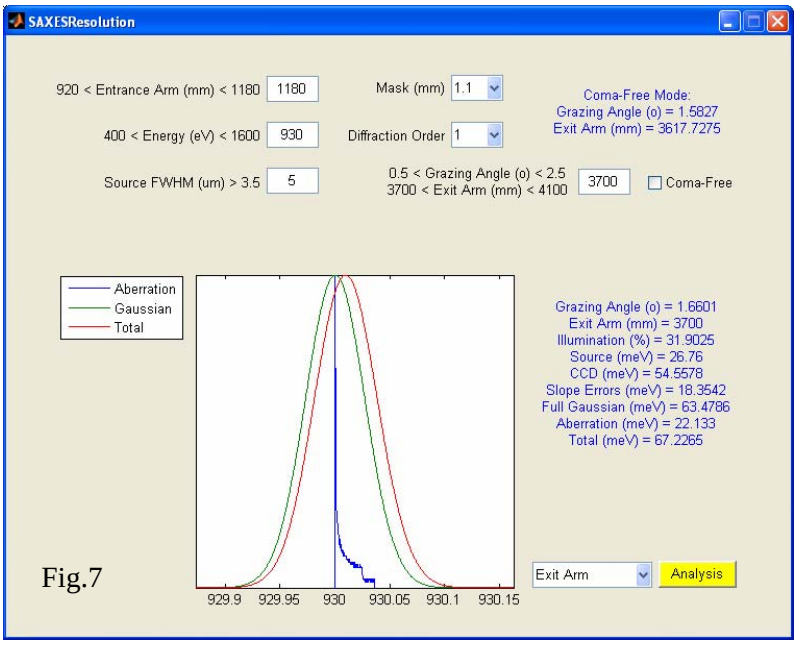

Fig.7